Acta Crystallographica Section C
Crystal Structure Communications
ISSN 0108-2701

The structural phase transition in SrV_6O_{11}

Yoshiaki Hata,[a]* Yasushi Kanke[b] and Eiji Kita[c]

[a]Department of Applied Physics, National Defense Academy, 1-10-20 Hashirimizu, Yokosuka, Kanagawa 239-8686, Japan, [b]Advanced Nano Materials Laboratory, National Institute for Materials Science, 1-1 Namiki, Tsukuba 305-0044, Japan, and [c]Department of Applied Physics, University of Tsukuba, Ibaraki 305-8537, Japan
Correspondence e-mail: hata@nda.ac.jp

Received 12 May 2010
Accepted 9 November 2010
Online 19 November 2010

Single-crystal X-ray diffraction and specific heat studies establish that strontium hexavanadium undecaoxide, SrV_6O_{11}, undergoes a $P6_3/mmc$ to inversion twinned $P6_3mc$ structural transition as the temperature is lowered through 322 K. The $P6_3/mmc$ and $P6_3mc$ structures have been determined at 353 K and at room temperature, respectively. For the room-temperature structure, seven of the ten unique atoms lie on special positions, and for the 353 K structure all of the seven unique atoms sit on special positions. The $P6_3/mmc$ to $P6_3mc$ structural phase transition, accompanied by a magnetic transition, is a common characteristic of AV_6O_{11} compounds, independent of the identity of the A cations.

Comment

A series of AV_6O_{11} compounds (A = Na, K, Sr, Ba, Pb; de Roy *et al.*, 1987; Kanke, 1999; Kanke *et al.*, 1991; Friese *et al.*, 2006; Mentre *et al.*, 1996) have generated interest because of their structural phase transitions, magnetic and transport properties (Kanke *et al.*, 1990, 1994; Uchida *et al.*, 1991, 2001; Mentre *et al.*, 2001). The crystal structures consist of hexagonal close-packed layers of A and O atoms, and three types of V atoms (Fig. 1). The $V1O_6$ octahedra form a Kagomé lattice by edge sharing. The $V2O_6$ octahedra form face-sharing dimers between the layers of the Kagomé lattice. The coordination of $V3O_5$ is a trigonal bipyramid.

While the AV_6O_{11} compounds show common characteristics in their paramagnetic states, they exhibit individual characteristics for their magnetically ordered states. In the paramagnetic states, each AV_6O_{11} shows one phase transition at a characteristic temperature, T_t. Above T_t, the compounds crystallize in the centrosymmetric hexagonal space group $P6_3/mmc$, and show Curie–Weiss paramagnetism. Below T_t, the compounds lose the centre of symmetry and show second-order transitions to hexagonal $P6_3mc$ (Kanke *et al.*, 1994). The $V1O_6$ octahedron forms a regular Kagomé lattice above T_t. It distorts to form a $V1O_6$ trimer with a regular triangular shape below T_t. Two $V2O_6$ octahedra forming a face-sharing dimer are crystallographically equivalent above T_t. Below T_t, they become inequivalent. V3 is no longer at the centre of the $V3O_5$ polyhedron below T_t. In the $P6_3mc$ form of AV_6O_{11}, V1 exhibits a spin gap behaviour with a spin-singlet ground state, while V2 and V3 possess magnetic moments (Uchida *et al.*, 2001). T_t values for KV_6O_{11} (Kanke, 1999), BaV_6O_{11} (Friese *et al.*, 2006) and PbV_6O_{11} (Kato *et al.*, 2001) are 190, 250 and 560 K, respectively.

As first reported, the room-temperature structure of SrV_6O_{11} was assigned to $P6_3/mmc$ with a relatively high R factor (Kanke *et al.*, 1992). The T_t = 320 K of SrV_6O_{11} exceeds room temperature, which suggests an incorrect assignment of the space group. We have pointed out briefly the existence of the $P6_3/mmc$ to $P6_3mc$ transition at 320 K (Hata *et al.*, 1999). Kato *et al.* studied the transition by X-ray powder diffraction. They refined the structures at 100 K in $P6_3mc$ and at 623 K in $P6_3/mmc$ (Kato *et al.*, 2001). However, we considered a single-crystal diffraction study to be indispensable for an accurate structural characterization of the acentric phase. In the present study, the crystal structure of SrV_6O_{11} was determined in detail both above T_t (353 K) and below T_t (room temperature, RT) by single-crystal X-ray diffraction. The transition temperature was determined precisely by a specific heat study.

At both room temperature and 353 K, diffraction data showed hexagonal symmetry and an extinction rule, $l \neq 2n$ absent for hhl, indicating possible space groups $P6_3/mmc$, $P\bar{6}2c$ and $P6_3mc$. $P6_3/mmc$ is centrosymmetric and gives a unique structural model. But the other two are acentric, and each gives a pair of single-domain models, (x, y, z) and $(-x, -y, -z)$, and one inversion twin model, $[(x, y, z) + (-x, -y, -z)]$.

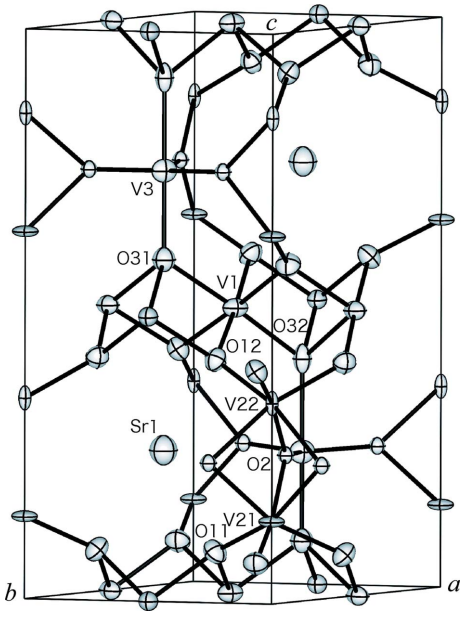

Figure 1
The crystal structure of SrV_6O_{11} at room temperature, shown with 99% probability displacement ellipsoids.

 doi:10.1107/S0108270110046299

To examine the possible models, reflections with $h \geq 0$, $k \geq 0$, $l \geq 0$, $|h| \leq |k|$, $2\theta < 90^\circ$, and those with $h \leq 0$, $k \leq 0$, $l \leq -1$, $|h| \leq |k|$, $2\theta \leq 90^\circ$ were collected at both temperatures using a four-circle diffractometer (Enraf–Nonius CAD-4) with Mo $K\alpha$ radiation. As the diffractometer is equipped with a scintillation counter, reflections that were too weak were regarded as unobserved. Thus, 185 of a total of 1284 reflections for room temperature, and 349 of 1290 reflections for 353 K were assigned as unobserved. The refinements did not use the unobserved data. The data, however, are of high resolution, 0.5 Å, and have what we consider sufficient completeness; for $2\theta < 50^\circ$, the completeness is 97.4% for room temperature and 92.9% for 353 K, even without the unobserved data. As a result, the model examinations give clear results as follows.

The models for room temperature were examined using 1093 Friedel-unaveraged reflections with $I > 1.5\sigma(I)$, applying the common weighting scheme of $1/\sigma(I)$. As shown in Table 1, the inversion twin $P6_3mc$ model gave trouble-free convergence and low enough R factors ($R_1 = 0.0231$, $wR_2 = 0.0515$, 44 parameters). However, all of the remaining models resulted in nonpositive definite atomic displacement parameter(s) and significantly higher R factors. Consequently, the twinned $P6_3mc$ model was selected. This clear differentiation of the results for the different models also indicates high enough quality of the specimen and high enough resolution of the diffraction data.

The models for 353 K were examined using 919 unaveraged reflections with $I > 1.5\sigma(I)$, applying the common weighting scheme of $1/\sigma(I)$. All seven models gave trouble-free convergence and low enough R factors ($R_1 = 0.0236$–0.0242, $wR_2 = 0.0511$–0.0526, 26–44 parameters). Consequently, there was no reason to choose any of the acentric space groups, and the $P6_3/mmc$ model, with the highest symmetry, was selected.

The room-temperature structure of SrV_6O_{11} had earlier been described by Kanke *et al.* (1992) using $P6_3/mmc$. They compared the $P6_3/mmc$ model, two single-domain models of $P\overline{6}2c$ and two single-domain models of $P6_3mc$, using 2031 unaveraged intensities. The $P6_3/mmc$ model, the better $P\overline{6}2c$ model and the better $P6_3mc$ model gave $R = 0.070$ with 24 parameters, $R = 0.069$ with 24 parameters and $R = 0.064$ with 35 parameters, respectively. The difference in the R factors was concluded to be insignificant, considering the numbers of parameters. Consequently, they chose the $P6_3/mmc$ model with the highest symmetry. However, the study did not examine the twin models for the two acentric space groups. None of the models was free from negative temperature factors, and anisotropic displacement parameters were not applied to O2 even in the final refinement. In the present study, in fact only the $P6_3mc$ model with inversion twinning is free of nonpositive definite displacement parameters, and this model clearly gives the best result among the seven models tested. We thus correct the previous report with this determination that SrV_6O_{11} crystallizes in $P6_3mc$ with inversion twinning at room temperature.

Between the two temperatures, *viz.* room temperature and 353 K, the specific heat of SrV_6O_{11} shows only one anomaly, at 322 K. Consequently, we conclude that the structural phase transition takes place at 322 K and coincides with the magnetic transition.

The structural refinements of the $P6_3mc$ forms of NaV_6O_{11} (Kanke *et al.*, 1994) and PbV_6O_{11} (Mentre *et al.*, 1996) converged promptly without applying twinning. Kanke (1999) suggested that this may be due to the small anomalous dispersion term for Na for Mo $K\alpha$ in NaV_6O_{11} or may suggest that the volume fraction ratio $(x, y, z) / (x, y, -z)$ is far from 1.0 in PbV_6O_{11} and/or in NaV_6O_{11}.

The $P6_3mc$ and $P6_3/mmc$ forms of SrV_6O_{11} are illustrated in Figs. 1 and 2, respectively. In both forms, the V1 ellipsoid is elongated towards the centre of the V1 trimer. V2 is nearly isotropic in the $P6_3/mmc$ form. In the $P6_3mc$ form, though, V21 is oblate, compressed into (001) and V22 is prolate along [001]. V3 shows extended displacement along [001] in the $P6_3/mmc$ form, but is rather isotropic in the $P6_3mc$ form.

For the $P6_3mc$ form, seven of the ten unique atoms lie on special positions, and for the $P6_3/mmc$ form, all of the seven unique atoms sit on special positions. In the centric structure, the $V1O_6$ octahedra form a regular Kagomé lattice with a uniform V1···V1 distance of 2.8887 (1) Å (Table 2). In the $P6_3mc$ phase, though, the Kagomé lattice distorts, with the $V1O_6$ octahedra forming a trimer with a regular triangular shape; and the V1···V1 distance separates into two types, *viz.* inter-trimer [2.9736 (6) Å] and intra-trimer [2.7966 (6) Å] (Table 3). It is noteworthy that SrV_6O_{11} shows a much smaller change in the V2···V2 distance with the phase transition, as compared to the other AV_6O_{11} compounds. In both the $P6_3/mmc$ and $P6_3mc$ forms, analogous V1—O distances show similar values, independent of the nature of A. On the other hand, in both forms the V2—O and the V3—O2 distances tend to be longer for divalent A cations and shorter for monovalent A.

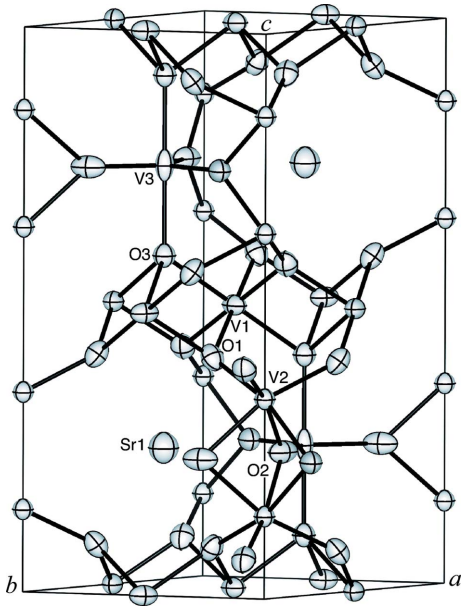

Figure 2
The crystal structure of SrV_6O_{11} at 353 K, shown with 99% probability displacement ellipsoids.

The $P6_3/mmc$ to $P6_3mc$ structural phase transition, accompanied by a magnetic transition, is a common characteristic of AV_6O_{11} compounds, independent of the A cations. The acentric form of SrV_6O_{11} shows features in common with the corresponding $P6_3mc$ forms of AV_6O_{11} (A = Na, K, Sr, Ba, Pb). Below T_t, the $V1O_6$ octahedron no longer forms a regular Kagomé lattice, but distorts to form a $V1O_6$ trimer with a regular triangular shape. A pair of the $V2O_6$ octahedra forming a face-sharing dimer at higher temperatures become inequivalent. V3 moves away from the centre of the $V3O_5$ polyhedron. The V1 trimer formation accompanying the structural transition is considered to be the factor that suppresses the paramagnetism below T_t.

Experimental

$Sr_2V_2O_7$ and V_2O_3 were mixed in a 1:5 molar ratio. The mixture was sealed in a platinum capsule and heated at 1073 K for 1 d and at 1473 K for 2 weeks, successively. Crystals of SrV_6O_{11} were hexagonal plates with principal faces {001}. Sizes were typically 0.2 mm across the plate and 0.1 mm in thickness.

Data collection at 353 K was achieved by blowing hot nitrogen gas onto the specimen. The temperature was calibrated by a chromel-alumel thermocouple with a water-ice standard. The specific heat of single-crystal SrV_6O_{11} was measured using a Quantum Design Physical Property Measurement System (PPMS). The temperature range of the measurements was from 2.4 to 350 K.

SrV_6O_{11} at 353 K

Crystal data

SrV_6O_{11}
M_r = 569.26
Hexagonal, $P6_3/mmc$
a = 5.7773 (1) Å
c = 13.0852 (3) Å
V = 378.234 (13) Å^3
Z = 2
Mo $K\alpha$ radiation
μ = 14.15 mm^{-1}
T = 353 K
0.31 × 0.14 × 0.08 mm

Data collection

Enraf–Nonius CAD-4 diffractometer
Absorption correction: Gaussian (*SDP*; B. A. Frenz & Associates Inc., 1985)
T_{min} = 0.413, T_{max} = 0.532
1290 measured reflections
645 independent reflections
447 reflections with $I > 1.5\sigma(I)$
R_{int} = 0.016
3 standard reflections
every 240 min
intensity decay: 0.7%

Refinement

$R[F^2 > 2\sigma(F^2)]$ = 0.021
$wR(F^2)$ = 0.054
S = 1.37
447 reflections
26 parameters
$\Delta\rho_{max}$ = 0.84 e Å^{-3}
$\Delta\rho_{min}$ = −0.81 e Å^{-3}

SrV_6O_{11} at room temperature

Crystal data

SrV_6O_{11}
M_r = 569.26
Hexagonal, $P6_3mc$
a = 5.7702 (1) Å
c = 13.0784 (3) Å
V = 377.109 (13) Å^3
Z = 2
Mo $K\alpha$ radiation
μ = 14.19 mm^{-1}
T = 295 K
0.31 × 0.14 × 0.08 mm

Data collection

Enraf–Nonius CAD-4 diffractometer
Absorption correction: Gaussian (*SDP*; B. A. Frenz & Associates Inc., 1985)
T_{min} = 0.382, T_{max} = 0.529
1284 measured reflections
1247 independent reflections
1065 reflections with $I > 1.5\sigma(I)$
R_{int} = 0.016
3 standard reflections
every 240 min
intensity decay: 0.4%

Refinement

$R[F^2 > 2\sigma(F^2)]$ = 0.022
$wR(F^2)$ = 0.055
S = 1.21
1065 reflections
44 parameters
$\Delta\rho_{max}$ = 0.97 e Å^{-3}
$\Delta\rho_{min}$ = −1.27 e Å^{-3}
Absolute structure: refinement of absolute structure parameter (Flack, 1983)
Flack parameter: 0.434 (7)

Structural parameters including one single-domain model or two inversion twin models, scale factors and one free parameter for extinction correction were refined with *SHELXL97* (Sheldrick, 2008).

Table 1
Results for refinement of different models for SrV_6O_{11} at room temperature.

Space group	Model	N_r[a]	N_P[b]	R_1	wR_2
$P6_3/mmc$	Unique[c]	1093	26	0.0574	0.1111
$P6_3mc$	(x, y, z)[d]	1093	43	0.0459	0.1002
$P6_3mc$	$(-x, -y, -z)$[d]	1093	43	0.0390	0.0832
$P6_3mc$	$(x, y, z)+(-x, -y, -z)$[e]	1093	44	0.0231	0.0515
$P\bar{6}2c$	(x, y, z)[f]	1093	32	0.0571	0.1110
$P\bar{6}2c$	$(-x, -y, -z)$[f]	1093	32	0.0571	0.1110
$P\bar{6}2c$	$(x, y, z)+(-x, -y, -z)$[g,h]	1093	33	0.0558	0.1100

Notes: (*a*) number of reflections; (*b*) number of parameters; (*c*) displacement parameters of V1 are negative; (*d*) displacement parameters of O2 are negative; (*e*) the volume fraction (x, y, z):$(-x, -y, -z)$ = 0.434 (7):0.566 (7); (*f*) displacement parameters of V1 and O2 are negative; (*g*) displacement parameters of V1, O1 and O2 are negative; (*h*) the volume fraction (x, y, z):$(-x, -y, -z)$ = 0.519:0.481 (72).

Table 2
Selected bond lengths (Å) for SrV_6O_{11} at 353 K.

Sr1—O1	2.7232 (13)	V2—O2	2.0423 (16)
Sr1—O2	2.892 (2)	V3—O2^{i}	1.810 (2)
V1—O1	1.9522 (9)	V3—O3	2.090 (2)
V1—O3	2.0438 (12)	V1—V1^{ii}	2.8887 (1)
V2—O1	1.9312 (14)	V2—V2^{iii}	2.7166 (9)

Symmetry codes: (i) $x-y, x, z+\frac{1}{2}$; (ii) $-x+y, -x+1, z$; (iii) $x, y, -z+\frac{1}{2}$.

Table 3
Selected bond lengths (Å) for SrV_6O_{11} at room temperature.

Sr1—O11	2.738 (2)	V22—O12	1.951 (2)
Sr1—O12	2.700 (2)	V22—O2	2.025 (3)
Sr1—O2	2.8887 (9)	V3—O2^{ii}	1.8057 (15)
V1—O11^{i}	1.9422 (18)	V3—O31	2.038 (4)
V1—O12	1.9598 (16)	V3—O32^{ii}	2.136 (3)
V1—O31	2.069 (2)	V1—V1^{iii}	2.7966 (6)
V1—O32	2.018 (2)	V1—V1^{iv}	2.9736 (6)
V21—O11	1.911 (2)	V21—V22	2.7151 (8)
V21—O2	2.063 (3)		

Symmetry codes: (i) $y, -x+y, z+\frac{1}{2}$; (ii) $x-y, x, z+\frac{1}{2}$; (iii) $-y+1, x-y, z$; (iv) $-x+y, -x+1, z$.

For both temperatures, data collection: *CAD-4* (Enraf–Nonius, 1981); cell refinement: *CAD-4*; data reduction: *SDP* (B. A. Frenz & Associates Inc., 1985); program(s) used to solve structure: *SHELXS97* (Sheldrick, 2008); program(s) used to refine structure: *SHELXL97* (Sheldrick, 2008); molecular graphics: *VESTA* (Momma & Izumi, 2008); software used to prepare material for publication: *SHELXL97*.

Supplementary data for this paper are available from the IUCr electronic archives (Reference: FA3226). Services for accessing these data are described at the back of the journal.

References

B. A. Frenz & Associates Inc. (1985). *SDP. Structure Determination Package*, 4th ed. Enraf–Nonius, Delft, The Netherlands.

Enraf–Nonius (1981). *CAD-4 Operations Software.* Enraf–Nonius, Delft, The Netherlands.

Flack, H. D. (1983). *Acta Cryst.* A**39**, 876–881.

Friese, K. & Kanke, Y. (2006). *J. Solid State Chem.* **179**, 3277–3285.

Hata, Y., Kanke, Y., Kita, E., Suzuki, H. & Kido, G. (1999). *J. Appl. Phys.* **85**, 4768–4770.

Kanke, Y. (1999). *Phys. Rev. B*, **60**, 3764–3776.

Kanke, Y., Izumi, F., Morii, Y., Akiba, E., Funahashi, S., Kato, K., Isobe, M., Takayama-Muromachi, E. & Uchida, Y. (1994). *J. Solid State Chem.* **112**, 429–437.

Kanke, Y., Izumi, F., Takayama-Muromachi, E., Kato, K., Kamiyama, T. & Asano, H. (1991). *J. Solid State Chem.* **92**, 261–272.

Kanke, Y., Kato, K., Takayama-Muromachi, E. & Isobe, M. (1992). *Acta Cryst.* C**48**, 1376–1380.

Kanke, Y., Takayama-Muromachi, E., Kato, K. & Matsui, Y. (1990). *J. Solid State Chem.* **89**, 130–137.

Kato, H., Kato, M., Yoshimura, K. & Kosuge, K. (2001). *J. Phys. Condens. Matter*, **13**, 9311–9333.

Mentre, O. & Abraham, F. (1996). *J. Solid State Chem.* **125**, 91–101.

Mentre, O., Kanke, Y., Dhaussy, A.-C., Conflant, P., Hata, Y. & Kita, E. (2001). *Phys. Rev. B*, **64**, 174404.

Momma, K. & Izumi, F. (2008). *J. Appl. Cryst.* **41**, 653–658.

Roy, M. E. de, Besse, J. P., Chevalier, R. & Gasperin, M. (1987). *J. Solid State Chem.* **67**, 185–189.

Sheldrick, G. M. (2008). *Acta Cryst.* A**64**, 112–122.

Uchida, Y., Onoda, Y. & Kanke, Y. (2001). *J. Magn. Magn. Mater.* **226**, 446–448.

Uchida, Y., Kanke, Y., Takayama-Muromachi, E. & Kato, K. (1991). *J. Phys. Soc. Jpn*, **60**, 2530–2533.